

Influence of hydrophilicity/hydrophobicity on adsorption/desorption of sulfanilic acid using amine-modified silicas and granular activated carbon

Waheeba A. Al-Amrani^a, M.A.K.M. Hanafiah^{b,*}, Poh-Eng Lim^c

^aDepartment of Chemistry, College of Science, Ibb University, Ibb, Yemen, email: alamraniwaheeba@gmail.com

^bFaculty of Applied Sciences, Universiti Teknologi MARA, 26400, Jengka, Pahang, Malaysia, email: makmh@uitm.edu.my

^cSchool of Chemical Sciences, Universiti Sains Malaysia, 11800 Penang, Malaysia, email: pelim04@yahoo.com

Received 16 September 2021; Accepted 2 January 2022

ABSTRACT

Different particle sizes of mono-amine modified silicas (MAMS) were synthesized using 3-aminopropyltriethoxysilane (3-APTES) to remove sulfanilic acid from its aqueous solutions. The synthesized adsorbents were characterized using a Fourier-transform infrared spectrophotometer and scanning electron microscope. The surface area, pore width, pore diameter, and pH_{PZC} were also measured. The adsorption/desorption behaviour of MAMS was investigated and compared to the commercial granular activated carbon (GAC). The experimental results showed the homogeneous distribution of the active sites on the MAMS surface compared to the heterogeneous distribution of the active sites on the GAC surface. The maximum sulfanilic acid (SA) adsorbed on GAC and MAMS adsorbents occurred at pH 3.5 (neutral pH of SA in distilled water) and equilibrium contact time of 1 h and 30 min, respectively. Kinetic studies showed that the pseudo-first-order model was well fitted to the adsorption of SA molecules on all the investigated adsorbents. The MAMS adsorbent displayed a rapid adsorption rate due to its high hydrophilicity character relative to the GAC adsorbent. Isotherm and desorption studies revealed that the interaction mechanisms of SA molecules on MAMS and GAC displayed different approaches based on the adsorbent surface characteristics. Desorption of SA-exhausted adsorbents was 100% and \approx 35% using distilled water for MAMS and GAC, respectively.

Keywords: Hydrophilicity/hydrophobicity; Adsorption; Modified silica; Granular activated carbon; Sulfanilic acid; Water treatment

1. Introduction

Environmental pollution caused by synthetic organic chemicals is a serious issue to address today to achieve good water quality. Sulfonated aromatic amines compounds are usually discharged into water bodies through industrial effluents. The main sources of these recalcitrant sulfonated aromatic amines contaminants are the manufacture and bio-degradation of dyestuffs, particularly azo dyes [1–3]. The azo dyes biodegradation can occur in two steps: (i) The first includes the reductive cleavage of $-\text{N}=\text{N}-$ moieties in

anaerobic conditions, leading to the creation of harmful sulfonated aromatic amines, for instance, amino benzene sulfonic acids, and (ii) The second comprises the aerobic biodegradation of the later compounds. The sulfonated aromatic amines contaminants are tough to biodegrade, although different bacterial strains can slowly biodegrade them under aerobic conditions [4,5]. As a result, sulfonated aromatic amines compounds are often found in the effluents of dyehouses and textile industries.

Sulfanilic acid (SA), or 4-aminobenzenesulfonic acid, is an example of a sulfonated aromatic amine widely used in

* Corresponding author.

producing azo dyes. In addition, food, dye, perfume, and pesticides are examples of industries that consume a large concentration of SA. As shown in Table 1, SA is a polar compound, has high chemical stability (bio-recalcitrance) and is highly soluble in water [2,6,7]. Its presence in water bodies can endanger aquatic lives; therefore, SA-contaminated waters must be treated appropriately. Remediation of SA-contaminated waters was done using different technologies such as biological treatments [2,8], electrochemical oxidation [6,9], membrane extraction [10], microwave irradiation [7], catalytic ozonation [11] and adsorption processes [12,13].

The adsorption process primarily removes contaminants from waters and wastewater, especially non-degradable compounds [14]. Granular activated carbons (GAC) are the most common adsorbents used to adsorb sulfonated aromatic amines [7,13,15]. However, GAC production is quite costly, and the exhausted GAC is hard to regenerate. Hence, other low-cost adsorbents with high adsorption capacity and high rate adsorption are sought. Silica gel is a much cheaper material, and it exhibits high thermal and chemical stability. Silica gel also shows good selectivity, swelling resistance and can be reused [16]. Thus, silica was modified with chelating agents to enhance adsorption performance for azo dyes [17], heavy metals [18,19], pesticides [20], and polycyclic aromatic hydrocarbons [21]. An extensive literature search found no work related to mono-amine modified silica adsorbent (MAMS) at different particle sizes in removing sulfonated aromatic amines from their aqueous solutions.

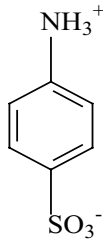
In this study, mono-amine modified silica (MAMS) at different particle sizes of 0.25–0.42 mm (40–60 mesh) and 0.063–0.1 mm (140–230 mesh) were synthesized using 3-aminopropyltriethoxysilane (3-APTES) to remove sulfanilic acid (SA) molecules, as a model of non-degraded sulfonated aromatic amine compounds, from aqueous solutions. The adsorption characteristics of SA molecules on the obtained silicas in distilled water were elucidated at different experimental conditions such as different pHs and different initial SA concentrations and compared to the commercial GAC particles. Mathematical kinetic and isotherm models were tested to calculate the adsorption rate and the adsorption capability of MAMS adsorbent for SA molecules at different particle sizes. The mechanism of SA interaction on the investigated adsorbents, namely MAMS and GAC, has also been clarified. Desorption of SA-exhausted adsorbents was studied using different eluents.

2. Experimental

2.1. Chemicals

3-aminopropyltriethoxysilane (3-APTES) of synthesis grade with >99% purity was purchased from Merck, Germany. Sulfanilic acid (SA) with >99% purity (Table 1) and silica gel with particle sizes of 0.25–0.42 mm (40–60 mesh) and 0.063–0.1 mm (140–230 mesh) were purchased from Aldrich, Germany. The GAC was a commercially available activated carbon (NORIT 830), a steam-activated wood-based carbon of particle size of 0.25–0.42 mm (40–60 mesh). Additional chemicals were of AR grade and were used as obtained.

Table 1
The chemical properties of sulfanilic acid (SA) molecule

Property	Value
Molecular formula	$\text{H}_3\text{NC}_6\text{H}_4\text{SO}_3$
Molecular mass	173.19 g/mol
Density	1.485 g/cm ³
Melting point	288°C
Acidity (pKa) in H ₂ O	3.23
Purity	>99%
λ_{max} at (pH = 3.5)	248
Structural formula	

2.2. Preparation of adsorbents

The MAMS particles were synthesized by modifying the surface of the commercial silica gel particles using 3-APTES as a silylating agent, and the detailed procedure has been described in previous work [17]. The synthesized MAMS adsorbent with two different particles was dehydrated at 120°C for 2 h. The adsorbent was sieved to 0.25–0.42 mm (40–60 mesh) and was labelled as MAMS1. Another fraction of 0.063–0.1 mm (140–230 mesh) was obtained and labelled as MAMS2 and kept in a desiccator. The GAC was sieved and separated to the size of 0.25–0.42 mm (40–60 mesh) and kept dry in an oven at 105°C overnight.

2.3. Characterization of adsorbents

The functional groups of MAMS1 and GAC were analyzed using a Fourier-transform infrared (FTIR) (Perkin Elmer, 2000, USA) spectrophotometer. The pore distribution, pore volume, pore diameter, specific surface area and total surface area were determined using an automatic sorption analyzer (Micromeritics, ASAP 2000, USA) for the investigated samples of MAMS1, MAMS2 and GAC. The surface morphology of the adsorbents, namely MAMS1 and GAC, was carried out using a scanning electron microscope (SEM) (Leo Supra 50 VP, Germany). The pH of zero point charge or pH_{PZC} of MAMS1 and GAC was regulated by the supposed pH drift technique [22,23].

2.4. Preparation of SA solution and concentration measurements

A standard solution (1,000 g/L) of SA was prepared and diluted to the desired concentrations using distilled water. The concentrations of SA were quantified using a UV-Vis spectrophotometer (Shimadzu, UV-2600, Japan) at λ_{max} of 248 nm. The amount of SA onto the adsorbents was determined using the following equation [15]:

$$q_e (\text{mg/g}) = \frac{(C_{\text{initial}} - C_{\text{final}}) \times V}{m} \quad (1)$$

where C_{initial} and C_{final} are the initial and final SA concentrations (mg/L), V is the volume (L) of the solution, and m is the mass (g) of adsorbent.

2.5. Adsorption experiments

2.5.1. Different initial pH of solutions

The effect of different initial pH values on the adsorption of SA onto MAMS1 and GAC particles with a particle size of 0.24–0.52 mm at 26°C was investigated. A weight of 0.10 g for each dry adsorbent was placed in 100 mL-conical flasks with a total working volume of 50 mL containing SA solution with a 100 and 300 mg/L concentration for MAMS1 and GAC, respectively. The desired pH was controlled using 2.0 M of HCl or NaOH solutions. Then, the contents were shaken at 200 rpm for 30 min for MAMS1 and 1 h for GAC at 26°C. The supernatant was separated, and the amount of SA adsorbed onto each adsorbent was calculated using Eq. (1).

2.5.2. Different contact time intervals

The mass of 0.10 g of each investigated adsorbent was placed in 100 mL conical flasks with a working volume of 50 mL containing SA of 100, 200 and 400 mg/L for MAMS1, MAMS2 and GAC, respectively. The solution was shaken at 200 rpm and 26°C, while the pH was kept at 3.5. The residual SA concentration (C_p) was determined spectrophotometrically at different time intervals until the equilibrium state was attained. The amount of SA adsorbed for each adsorbent at different time intervals was calculated using Eq. (1).

2.5.3. Different initial SA concentrations

Different initial SA concentrations were mixed with the investigated adsorbents to evaluate their maximum experimental adsorption capacities. Exactly 0.10 g of the modified silica with different particle sizes and GAC adsorbent was added into 100 mL conical flasks with a working volume of 50 mL. The SA concentration was varied from 10 to 400 mg/L for MAMS1, 50 to 600 mg/L for MAMS2 and 50 to 800 mg/L for GAC. The samples were shaken at 200 rpm, pH 3.5 and 30 min for modified silicas and 1 h for GAC at 26°C. The remaining SA concentration, C_p was determined spectrophotometrically.

2.6. Desorption study

Initially, a dosage of 0.50 g of each adsorbent, namely MAMS1 and GAC (particle size of 0.24–0.52 mm), was loaded with 200 and 800 mg/L initial SA concentrations, respectively with a total volume of 250 mL. The contents were agitated at 200 rpm for 30 min for MAMS1 and 1 h for GAC to attain the equilibrium state. The exhausted adsorbent was discarded, and the remaining SA, C_e in the supernatant was measured spectrophotometrically. The maximum SA

adsorbed on each adsorbent, q_e , was calculated using Eq. (1). Then, each exhausted adsorbent was mixed with different media separately, namely distilled water, NaOH (pH = 8), and a mixture of different salts solutions of (40 mg/L) CaCl_2 , (11 mg/L) FeCl_3 , (50 mg/L) MgSO_4 and (172 mg/L) NH_4Cl . The total pH of this mixture was 6.62 in a series of flasks of a total volume of 700 mL. The contents were shaken at 120 rpm and 26°C. The time courses of SA concentration, C_e desorbed from each loaded adsorbent using different media were monitored until desorption equilibrium was attained. The SA desorbed from each exhausted adsorbent at the equilibrium contact time, C_e was measured spectrophotometrically. The desorption percentage (%) was calculated as follows:

$$\text{Desorption (\%)} = \frac{C_e V}{q_e m} \times 100 \quad (2)$$

where C_e (mg/L) is the maximum azo dye desorbed from the SA-exhausted adsorbent in the bulk solution, q_e (mg/g) is the maximum adsorption capacity of SA on the adsorbent, m is the dosage (g) of the exhausted adsorbent, and V is the working volume (L) of the eluent used in the desorption study.

3. Results and discussion

3.1. Characterization of adsorbents

FTIR spectra of the surface functional groups for GAC, unmodified silica gel, and MAMS1 adsorbents (particle size of 0.25–0.42 mm) are presented in Fig. 1a–c. For comparison purposes, the results obtained for silica gel (0.25–0.42 mm) are also included. The spectrum of GAC (Fig. 1a) did not show any specific surface characteristic bands, which means there were no identifiable surface groups present on the GAC surface. In contrast, the spectra of unmodified silica gel and MAMS1 particles presented some significant surface characteristic bands (Fig. 1b and c). The spectrum of unmodified silica gel shows a broad band at $3,446 \text{ cm}^{-1}$ which could be assigned to the $\nu(\text{O-H})$ stretching vibration mode of hydroxyl functional groups originating from silica inherently present in silica gel and the adsorbed water on the surface of the adsorbent. The very strong absorption peak at $1,048 \text{ cm}^{-1}$ portrays the functional group of siloxane backbone $\nu(\equiv\text{Si-O-Si}\equiv)$. The medium absorption peak of 811 cm^{-1} was assigned to tetrahedron ring $\nu(\equiv\text{SiO}_4)$ [17]. The spectrum of MAMS1 displays virtually the same surface characteristic bands as those of unmodified silica (Fig. 1c). However, the intensity of the free silanol group at 973 cm^{-1} disappeared in the MAMS1 adsorbent due to the formation of a new bond of $(\equiv\text{Si-O-C}\equiv)$, as shown in Fig. 1c. Furthermore, the spectrum of the MAMS1 is characterized by the presence of two weak and short absorption bands at $2,937 \text{ cm}^{-1}$ that can be assigned to the stretching frequency of $\nu(\text{=CH}_2)$. The above behaviour provides good evidence for the successful modification process of silica gel particles.

The physical characteristics of the investigated adsorbents are presented in Table 2. It was observed that the Brunauer–Emmett–Teller (BET) surface area, pore width and pore diameter of the free silica gel adsorbent were

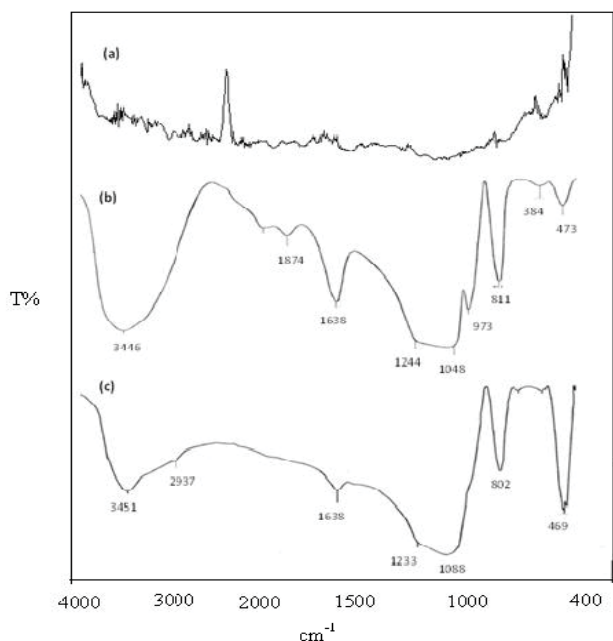


Fig. 1. FTIR spectra of 0.25–0.42 mm particle size of (a) GAC, (b) unmodified silica gel and (c) MAMS1.

reduced after modification of silica surface with 3-APTES. The micropore area in MAMS1 (0.25–0.42 mm) was found to be absent compared to that of the free silica gel (0.25–0.42 mm), leading to particles with no porosity and decreased surface area (Table 2). These differences are attributed to the presence of the pendant organo-functional groups, which obstructed the contact of nitrogen molecules to the original construction of silica gel [17]. On the other hand, the BET surface area for MAMS2 (0.063–0.100 mm) of 428.38 m²/g was approximately analogous to the free silica gel, even though the micro-pore area of MAMS2 was absent

(Table 2). This is due to the decrease in the particle size of silica gel from 0.25–0.42 mm to 0.063–0.100 mm. Table 2 shows that the commercial GAC adsorbent of 0.25–0.42 mm has the highest BET surface area of 725 m²/g, the micro-pore volume of 0.2451 cm³/g and the smallest pore diameter of 17.54 Å compared to the other investigated adsorbents. The high microporosity of GAC was evident by determining the ratio between the total micro-pore surface area (528 m²/g) to the total BET surface area (725 m²/g), which was found to be 73%.

The SEM images for the morphology of the investigated adsorbents of particle size 0.25–0.42 mm are shown in Fig. 2a–c in magnification of 10,000×. Fig. 2a shows that the GAC surface had rough regions containing many cracks and cavities, which exposed its inner area and offered an appropriate surface for adsorption. Visually, the modification of silica gel particles did not change the morphology of the surface matrix. Silica gel before and after modification presented an amorphous and rigid property, and there was no evidence of the porosity, as indicated in Fig. 2b and c. However, Fig. 2c shows that the surface of MAMS1 particles appeared to have a smoother surface than the unmodified silica gel (Fig. 2b).

The pH_{PZC} of the adsorbent is a critical value for determining the net charge (positive or negative) carried on the adsorbent surface during the adsorption process. Thus, the pH_{PZC} value for each adsorbent was estimated according to the drift method [22] and found to be 7.75, 6.81 and 6.88 for GAC, MAMS1 and MAMS2, respectively (Table 2).

3.2. Adsorption studies

3.2.1. Different initial pH of solutions

The results of SA adsorption onto GAC and MAMS1 at different pH for particle sizes of 0.25–0.42 mm are shown in Fig. 3. The adsorption behaviour of SA was similar from pH 1 to pH 8 for both adsorbents. Also, the

Table 2
The physicochemical properties of the investigated adsorbents

Property	Particle size, (mm)	Adsorbent		
		GAC	Silica gel	MAMS
BET surface area (m ² /g)	0.25–0.42	725.33	455.57	243.68
	0.063–0.100	–	–	428.38
Pore volume (cm ³ /g)	0.25–0.42	0.42	0.74	0.57
	0.063–0.100	–	–	0.57
Micropore volume (cm ³ /g)	0.25–0.42	0.25	0.00	0.00
	0.063–0.100	–	–	0.00
Micropore area (m ² /g)	0.25–0.42	527.48	9.28	00.00
	0.063–0.100	–	–	00.00
Pore width (Å)	0.25–0.42	–	–	93.82
	0.063–0.100	–	–	53.54
Pore diameter (Å)	0.25–0.42	17.54	65.27	69.45
	0.063–0.100	–	–	48.36
pH_{PZC}	0.25–0.42	7.75	–	6.81
	0.063–0.100	–	–	6.88

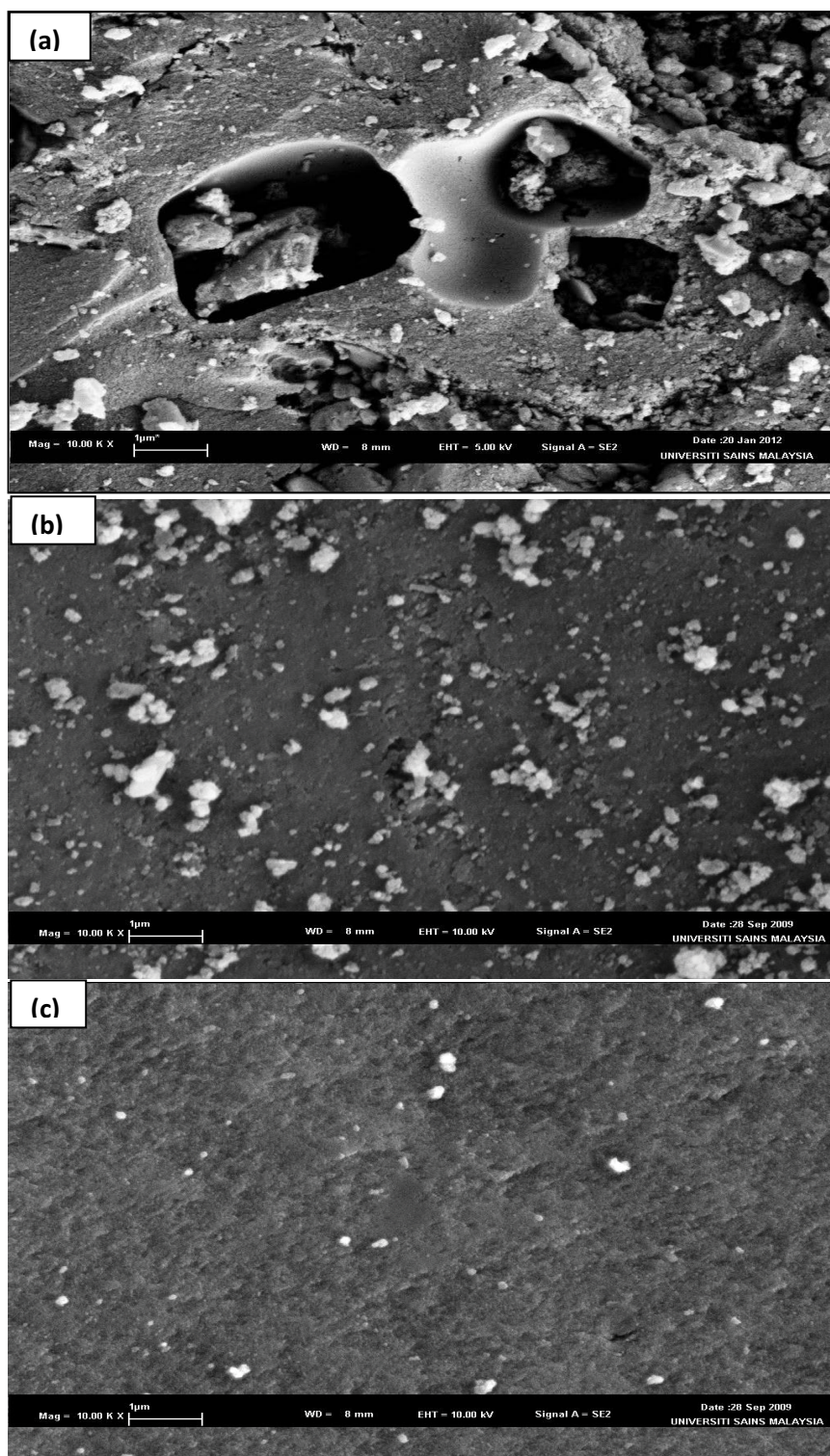


Fig. 2. SEM images in magnification of 10,000× for 0.25–0.42 mm particle size of (a) GAC, (b) silica gel and (c) MAMS1.

adsorption of SA molecules on GAC and MAMS1 showed a maximum at pH 3.5 (neutral pH of SA in water). This is attributed to the electrostatic attraction between the positively-charged protonated groups on both adsorbents ($\text{pH} < \text{pH}_{\text{PZC}}$, Table 2) and the negatively-charged sulfonate

groups ($-\text{SO}_3^-$) on SA molecules. It was reported that the optimal association of SA molecules at this acidity region ($\text{pK}_a = 3.23$) where SA is 87.1% in anionic form (negative charge is on the sulfonated group) and 12.9% in zwitterion form where negative charge is on sulfonate group and

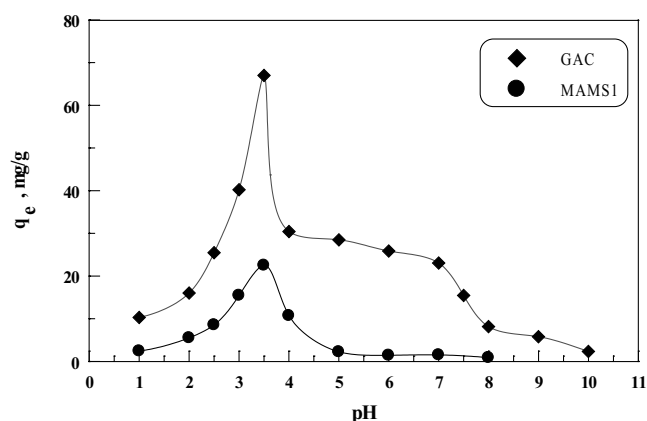


Fig. 3. pH effect on SA adsorption onto GAC and MAMS1 (0.25–0.42 mm particle size; the adsorbent weight of 0.1 g, 100 and 300 mg/L of SA concentrations for MAMS1 and GAC, respectively, 200 rpm, temperature of 26°C).

positive charge is on ammonium group [15]. Fig. 3 also shows that the adsorption behaviour of SA on GAC was relatively similar in the range of pH 4 to pH 7. In contrast, the amount of SA adsorbed onto MAMS1 at the same pH range was found to be drastically decreased. This reveals that electrostatic attraction is not the only mechanism for the SA adsorption onto GAC. Activated carbons can also interact with SA molecules via dispersive interactions, hydrogen bonding and hydrophobic-hydrophobic mechanisms [13], as can be seen in Fig. 4. On the other hand, the significant decline in SA adsorption onto GAC under basic conditions ($\text{pH} \geq 8$) might be characterized by electrostatic repulsion between the negatively-charged groups on the GAC ($\text{pH} > \text{pH}_{\text{pzc}}$, Table 2) and sulfonate group on SA molecule. It has been reported that in a strongly basic medium, the SA molecule is present in an anionic form with a sole negative charge on the sulfonate group [15].

3.2.2. Different contact time intervals

Different contact time intervals were studied for the adsorption of SA molecules on GAC, MAMS1 and MAMS2. The amount of SA molecules adsorbed on each adsorbent vs. contact time was plotted and shown in Fig. 5a and b. Fig. 5a shows that the time requisite for achieving the adsorption equilibrium of SA on GAC was about 1 h which is noticeably longer than that for MAMS1 of only 30 min at the same particle size of 0.25–0.42 mm. The long contact time for GAC is most likely attributed to the high micro-porosity of GAC compared to MAMS1 (Table 2).

Inspection of Fig. 5a and b shows that the required contact time to attain the adsorption equilibrium state decreased significantly from 30 min and 7 min when the particle size of modified silica decreased from 0.25–0.42 mm (MAMS1) to 0.063–0.1 mm (MAMS2). This may be attributed to decreased diffusion resistance to mass transfer when the adsorbent particle size decreased. Moreover, it can be perceived that the adsorption capacity of SA molecules on the GAC adsorbent is higher than that for MAMS1 and MAMS2 adsorbents. It was attributed to

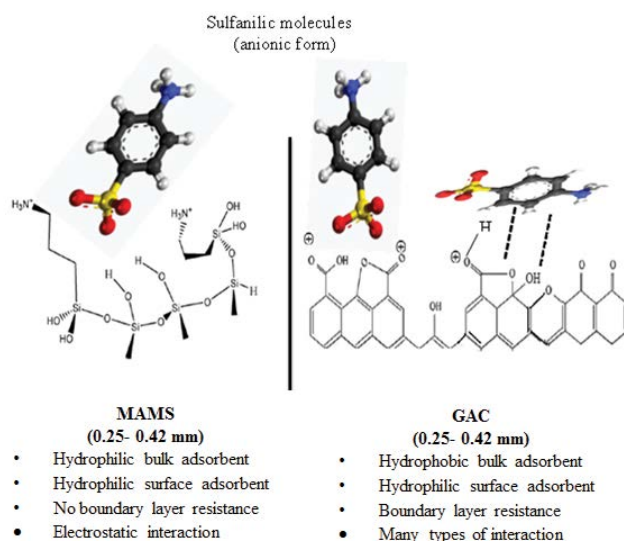


Fig. 4. Mechanism of the interaction between SA molecules (anionic form) with (a) MAMS1 and (b) GAC at pH 3.5.

the BET of GAC of 725.33 m^2/g , which is higher than for MAMS1 of 243.68 m^2/g , and MAMS2 of 428.38 m^2/g .

3.2.3. Different initial SA concentrations

Different initial concentrations of SA were investigated to study their effect on the adsorption process of GAC, MAMS1 and MAMS2. The amount adsorbed at equilibrium, q_e for SA vs. different initial concentrations (C_i) of SA was plotted and shown in Fig. 6. Generally, the experimental results in Fig. 6 exhibit that the adsorption capacities of GAC, MAMS1 and MAMS2 for SA molecules increased with the increase of the initial SA concentration until reaching the plateau. Moreover, it is noted that the initial SA concentration required to attain the plateau value of the amount adsorbed for GAC adsorbent of particle size of 0.25–0.42 mm was higher than that for MAMS1 and MAMS2 adsorbents (Fig. 6). This is attributed to the high surface area of GAC particles and their high porosity (Table 2).

3.3. Kinetic study

The adsorption data in Fig. 5a and b were treated in line with the non-linear kinetics models of the pseudo-first [Eq. (3)] and pseudo-second-order [Eq. (4)] models [24]:

$$q_t = q_e [1 - \exp(-k_1 t)] \quad (3)$$

$$q_t = \frac{ht}{1 + k_2 q_e t} \quad (4)$$

where q_e and q_t refer to the amount of SA adsorbed (mg/g) at equilibrium and at time t (min), k_1 is the overall rate constant of pseudo-first-order reaction (min^{-1}), h is the initial rate constant, k_2 is the overall rate constant of the pseudo-second-order reaction ($\text{g}/\text{mg} \cdot \text{min}$). MATLAB 7.5.0 was

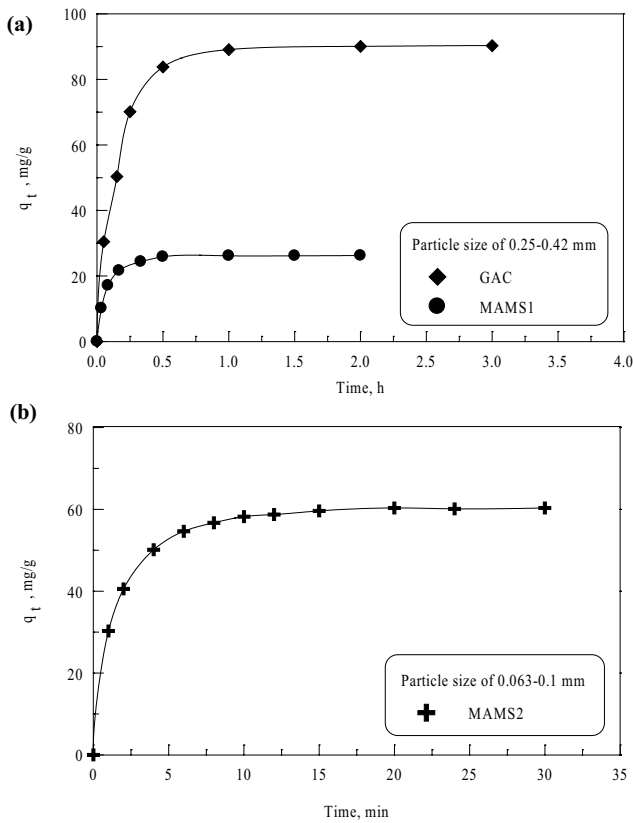


Fig. 5. Effect of contact time on adsorption of SA on (a) MAMS1 and GAC and (b) MAMS2 (SA concentrations of 100, 200, 400 mg/L for MAMS1, MAMS2 and GAC, respectively, pH 3.5, 200 rpm and temperature of 26°C).

used to fit the experimental data to the above two models. The kinetic constants were computed from the non-linear regression for each model and are given in Table 3. The results show that the pseudo-first-order model has good agreement with the experimental kinetic data based on satisfactory compliance obtained between the computed and the experimental values of q_e and the high regression correlation coefficients of $R^2 > 0.98$. This indicates that the possible adsorption rate-determining step is boundary layer resistance (external mass transfer). Therefore, the evaluation of k_1 values shows a noteworthy difference between adsorbents, and the values were in the sequence of MAMS1 > GAC > MAMS2. This means that MAMS1 could more quickly adsorb much higher SA during short exposure than GAC and MAMS2. These differences in k_1 values are due to (1) the differences in the pore diameter as seen in Table 2, in which the pore diameter sequence follows MAMS1 > MAMS2 > GAC and (2) the differences in the hydrophilicity/hydrophobicity of the adsorbent particles. For MAMS1 and GAC of 0.25–0.42 mm particle size, MAMS1 is a hydrophilic adsorbent (siloxane backbone of $\equiv\text{Si}-\text{O}-\text{Si}\equiv$ and positive amino-groups on the surface), as can be seen in Fig. 4. It implies less boundary layer resistance for the external mass transfer of anionic SA molecules from the bulk solution to the adsorbent particles. On the other hand, the hydrophobicity of GAC particles (carbon

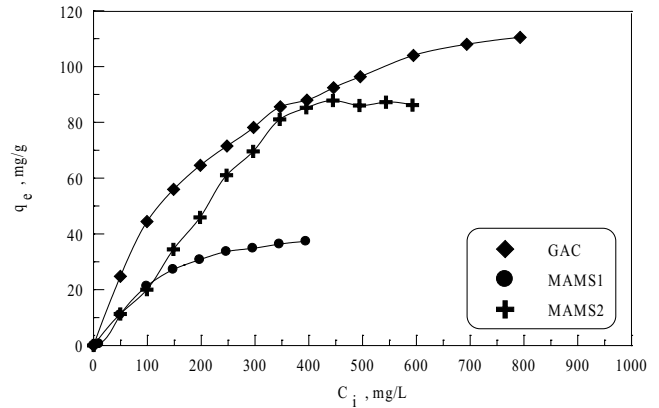


Fig. 6. Adsorption of SA onto GAC, MAMS1 and MAMS2 at different initial concentrations of SA (200 rpm, pH 3.5, contact time of 30 min and 1 h for modified silica and GAC, respectively, temperature of 26°C).

backbone of $-\text{C}-\text{C}-$) beside the narrow pore diameter of GAC, Table 2, increase the boundary layer resistance, resulting in the external mass transfer of the anionic SA molecules from the bulk solution to the GAC adsorbent is slow.

3.4. Isotherm study

The adsorption data of Fig. 6 were treated according to the non-linear Langmuir (Eq. 5) and Freundlich models [Eq. (6)] [13]:

$$q_e = q_{\max} \left(\frac{K_L C_e}{1 + K_L C_e} \right) \quad (5)$$

$$q_e = K_F C_e^{1/n} \quad (6)$$

where C_e is the equilibrium concentration of SA (mg/L), q_e is the adsorption capacity at equilibrium state (mg/g), q_{\max} is the theoretical maximum adsorption capacity (mg/g), K_L is the Langmuir isotherm constant which is related to the strength of adsorbent/adsorbate interaction (L/mg), K_F and n are the Freundlich constants related to the adsorption capacity and intensity, respectively. The Langmuir and Freundlich constants were calculated from the non-linear regression for each model at 26°C and are reported in Table 4. The results showed that the Freundlich equation was better than the Langmuir equation for SA adsorption onto GAC according to their correlation coefficients of 0.914 and 0.799, respectively. It is probably due to the heterogeneous distribution of active sites on GAC adsorbent. Conversely, SA adsorption onto MAMS1 and MAMS2 were fitted well to the Langmuir isotherm model (Table 4) based on their correlation coefficients of 0.973 and 0.915, respectively. This implies the homogeneous distribution of active sites on the surface of MAMS1 and MAMS2 with a better extent in the case of the former. The difference in the values of K_F and n for GAC and both modified silica adsorbents refers to the different binding strength of SA with the functional groups onto GAC and amino-groups on the surface of both silicas.

Table 3
Non-linear kinetic models of SA adsorption on the investigated adsorbents at 26°C

Adsorbent	Particle size, (mm)	$q_{e,exp}$ (mg/g)	Pseudo-first-order			Pseudo-second-order			
			$q_{e,cal}$ (mg/g)	k_1 (1/min)	R^2	h	$q_{e,cal}$ (mg/g)	k_2 (g/mg min)	R^2
GAC	0.25–0.42	90.28	89.27	6.17	0.9921	879.2	28.16	0.323	0.9905
MAMS1	0.25–0.42	26.22	25.69	13.02	0.9936	539.3	20.66	0.957	0.9963
MAMS2	0.063–0.100	60.33	58.66	0.604	0.9883	58.48	3.605	0.255	0.9988

Table 4
Non-linear isotherm models of SA adsorption on the investigated adsorbents at 26°C

Adsorbent	Particle size, (mm)	Langmuir				Freundlich			
		$q_{max,cal}$ (mg/g)	K_L (L/mg)	R_L	R^2	n	K_F (L/mg)	R^2	
GAC	0.25–0.42	108.10	0.025 ± 0.002	0.286	0.799	3.92 ± 0.00	22.01 ± 0.12	0.914	
MAMS1	0.25–0.42	52.70	0.0103 ± 0.002	0.493	0.973	1.88 ± 0.19	2.06 ± 0.46	0.924	
MAMS2	0.063–0.100	139.90	0.0102 ± 0.001	0.658	0.915	1.86 ± 0.22	3.91 ± 0.63	0.844	

Furthermore, the value of K_L for SA adsorption onto GAC is three times higher of MAMS1 and MAMS2. This emphasizes other types of interaction between SA molecules and the active adsorption sites on the GAC surface, as seen in Fig. 4. Meanwhile, the values of K_L for both modified silica, namely MAMS1 and MAMS2, showed no significant difference as the electrostatic attraction is the dominant interaction between SA molecules and amino groups on the surface of modified silica at pH 3.5.

The dimensionless constant or equilibrium factor parameter was calculated based on the following relationship [25]:

$$R_L = \frac{1}{1 + K_L C_0} \quad (7)$$

where C_0 is the initial concentration of SA (mg/L). The value of R_L indicates the nature of adsorption isotherm; irreversible ($R_L = 0$), favorable ($0 < R_L < 1$), and unfavorable ($R_L = 1$). As shown in Table 4, the calculated values of R_L were found between 0 and 1. This indicates that the adsorption of SA on all the investigated adsorbents is favourable from aqueous solutions under the used conditions in this study.

3.5. Desorption

Desorption of SA molecules from MAMS1 and GAC of particle size 0.25–0.42 mm was investigated at different media, namely distilled water, a mixture of different salts and NaOH (pH = 8). The desorption percentage vs. time was plotted and are presented in Fig. 7. The results showed that the desorption of SA from MAMS1 was considerably higher than from GAC in all the studied media. The desorption percentage of SA from MAMS1 was found to be 100% compared to that from GAC which was found to be $\approx 35\%$ using the investigated elutions. It is confirmed the differences in the binding mechanisms between MAMS and GAC. There is a significant contribution of

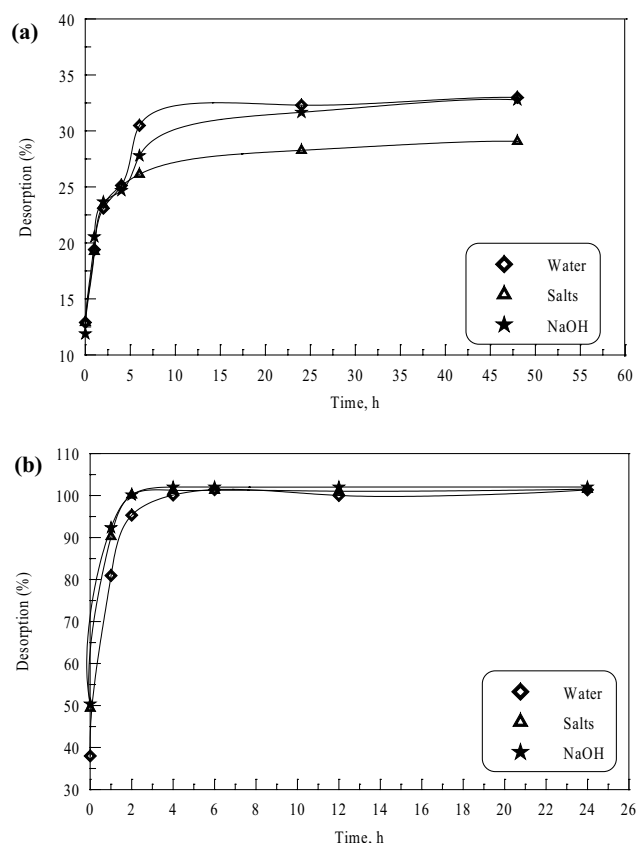


Fig. 7. Desorption of SA from the exhausted adsorbents (a) GAC and (b) MAMS1 using different eluents at 200 rpm and 26°C.

the non-electrostatic interactions besides the electrostatic attraction in the adsorption mechanism of SA onto the GAC surface compared to the electrostatic attraction in the adsorption of SA onto modified silica (Fig. 4). Besides, the time required to attain SA desorption equilibrium

Table 5
Three cycles adsorption/desorption of SA using the investigated adsorbents

Adsorbent	Cycle	Sulfanilic acid (SA)	
		Adsorption capacity, (mg/g)	Desorption, (%)
MAMS1	1	30	100
	2	28	97
	3	25	97
GAC	1	90	35
	2	88	33
	3	86	33

from SA-exhausted MAMS1 (Fig. 7b) was much shorter than GAC in all the investigated media. Three adsorption/desorption cycles were run using only distilled water for MAMS1 and GAC, and the data were presented in Table 5. The results showed a similar adsorption/desorption cycles trend for MAMS1 and GAC adsorbents. The adsorption capacities and percentage of desorption noticeably did change over three cycles of adsorption/desorption.

4. Conclusion

Amine-modified silicas, namely MAMS1 and MAMS2, were obtained using 3-APTES to remove sulfanilic acid from its aqueous solutions. The adsorption/desorption behaviour of amine-modified silica was compared to GAC particles. The amount of SA molecules adsorbed on the investigated adsorbent was at pH 3.5 (natural pH of SA in distilled water). Kinetic studies revealed that the adsorption of SA molecules on all the investigated adsorbents, namely MAMS1, MAMS2 and GAC, followed the pseudo-first-order model. Moreover, the SA adsorption rate-determining step on modified silicas and GAC was controlled by boundary layer resistance due to the differences in hydrophilicity/hydrophobicity characters of the investigated adsorbents. Mathematical isotherm studies showed that SA molecules' adsorption on amine-modified silicas followed the Langmuir model, whereas the Freundlich model was well fitted to SA adsorption on GAC. Active sites on modified silica surfaces were homogeneously distributed while they were heterogeneously distributed on the GAC surface. Isotherm and desorption studies showed that electrostatic attraction is the dominant interaction between SA molecules and amine groups on the surface of modified silicas. At the same time, other significant contributions besides electrostatic attraction were found in the adsorption mechanism of SA onto the GAC surface. Desorption of SA from the amine-modified silicas was easily done using distilled water, reaching an efficiency of 100% compared to GAC of ~35% over three cycles. It is evident that monoamine-modified silicas can be used for efficient, simple, and inexpensive removal of sulfanilic acid from aqueous solutions.

Conflicts of interest

The authors have no conflicts of interest to declare.

Acknowledgements

Waheeba A. Al-Amrani requests to thank Ibb University, Yemen and Universiti Sains, Malaysia, for the financial support.

References

- [1] W.A. Al-Amrani, P.-E. Lim, C.-E. Seng, W.S. Wan Ngah, Operational factors affecting the bioregeneration of monoamine modified silica loaded with Acid Orange 7, *Water Res.*, 46 (2012) 6419–6429.
- [2] R. Pereira, L. Pereira, F.P. van der Zee, M.M. Alves, Fate of aniline and sulfanilic acid in UASB bioreactors under denitrifying conditions, *Water Res.*, 45 (2011) 191–200.
- [3] R.T. Kapoor, M. Danish, R.S. Singh, M. Rafatullah, H.P.S. Abdul Khalil, Exploiting microbial biomass in treating azo dyes contaminated wastewater: mechanism of degradation and factors affecting microbial efficiency, *J. Water Process Eng.*, 43 (2021) 102255, doi: 10.1016/j.jwpe.2021.102255.
- [4] W.A. Al-Amrani, P.E. Lim, C.E. Seng, W.S. Wan Ngah, Bioregeneration of mono-amine modified silica and granular activated carbon loaded with Acid Orange 7 in batch system, *Bioresour. Technol.*, 118 (2012) 633–637.
- [5] W.A. Al-Amrani, P.E. Lim, C.E. Seng, W.S. Wan Ngah, Effects of co-substrate and biomass acclimation concentration on the bioregeneration of azo dye-loaded mono-amine modified silica, *Bioresour. Technol.*, 143 (2013) 584–591.
- [6] J. Zheng, K. Yan, Z. Wu, M. Liu, Z. Wang, Effective removal of sulfanilic acid from water using a low-pressure electrochemical RuO₂-TiO₂@Ti/PVDF composite membrane, *Front. Chem.*, 6 (2018) 395–405.
- [7] W. Ming-Chi, W. Kai-Sung, C. Lin, H. Tung-En, L. Yan-Ning, T. Chen-Ting, C. Jyh-Cheng, C. Shih-Hsien, Rapid regeneration of sulfanilic acid-sorbed activated carbon by microwave with persulfate, *Chem. Eng. J.*, 193–194 (2012) 366–371.
- [8] G. Chen, K.Y. Cheng, M.P. Ginige, A.H. Kaksonen, Aerobic degradation of sulfanilic acid using activated sludge, *Water Res.*, 46 (2012) 145–151.
- [9] A. El-Ghenymy, J.A. Garrido, F. Centellas, C. Arias, P.L. Cabot, R.M. Rodriguez, E. Brillas, Electro-Fenton and photoelectro-Fenton degradation of sulfanilic acid using a boron-doped diamond anode and an air diffusion cathode, *J. Phys. Chem. A*, 116 (2012) 3404–3412.
- [10] Y. Wang, G. Luo, W. Cai, Y. Wang, Y. Dai, Membrane extraction for sulfanilic acid removal from waste water, *Sep. Sci. Technol.*, 37 (2002) 1163–1177.
- [11] P.C.C. Faria, J.J.M. Órfão, M.F.R. Pereira, Catalytic ozonation of sulfonated aromatic compounds in the presence of activated carbon, *Appl. Catal., B*, 83 (2008) 150–159.
- [12] C.B. Vidal, A.L. Barros, C.P. Moura, A.C. de Lima, F.S. Dias, L.C. Vasconcellos, P.B. Fachine, R.F. Nascimento, Adsorption of polycyclic aromatic hydrocarbons from aqueous solutions by modified periodic mesoporous organosilica, *J. Colloid Interface Sci.*, 357 (2011) 466–473.
- [13] P.C.C. Faria, J.L. Figueiredo, M.F.R. Pereira, Adsorption of aromatic compounds from the biodegradation of azo dyes on activated carbon, *Appl. Surf. Sci.*, 154 (2008) 3497–3503.
- [14] Z.U. Zango, N.S. Sambudi, K. Jumbri, A. Ramli, N.H.H. Abu Bakar, B. Saad, M.N. Rozaini, H.A. Isiyaka, A.M. Osman, A. Sulieman, An overview and evaluation of highly porous adsorbent materials for polycyclic aromatic hydrocarbons and phenols removal from wastewater, *Water*, 12 (2020) 1–40.
- [15] O. Duman, E. Ayranci, Adsorption characteristics of benzaldehyde, sulphanyl acid, and phenolsulfonate from water, acid, or base solutions onto activated carbon cloth, *Sep. Sci. Technol.*, 41 (2006) 3673–3692.
- [16] P.K. Jal, B.K. Mishra, Chemical modification of silica surface by immobilization of functional groups for extractive concentration of metal ions, *Talanta*, 62 (2004) 1005–1028.
- [17] A.M. Donia, A.A. Atia, W.A. Al-Amrani, A.M. El-Nahas, Effect of structural properties of acid dyes on their adsorption

- behaviour from aqueous solutions by amine modified silica, *J. Hazard. Mater.*, 161 (2009) 1544–1550.
- [18] A.A. Atia, A.M. Doria, W.A. Al-Amrani, Effect of amine type modifier on the uptake behaviour of silica towards mercury(II) in aqueous solution, *Desalination*, 246 (2009) 257–274.
- [19] H. Ghaforinejad, H. Mazaheri, A.H. Joshaghani, A. Marjani, Study on novel modified large mesoporous silica FDU-12/ polymer matrix nanocomposites for adsorption of Pb(II), *PLoS One*, 16 (2021) 1–16.
- [20] M. Andrunik, T. Bajda, Removal of pesticides from waters by adsorption: comparison between synthetic zeolites and mesoporous silica materials. A review, *Materials*, 14 (2021) 1–38.
- [21] J. Regan, J. Dolores, M. Lepore, M. Gualano, J. Badson, A. Zimnoch, J.F. Capitani, J. Fan, Modified silica gels as recyclable adsorbents of aqueous polycyclic aromatic hydrocarbons, *Green Chem. Lett. Rev.*, 12 (2019) 434–443.
- [22] M.V. Lopez-Ramon, F. Stoeckli, C. Moreno-Castilla, F. Carrasco-Marín On the characterization of acidic and basic surface sites on carbons by various techniques, *Carbon*, 37 (1999) 1215–1221.
- [23] P.C.C. Faria, J.J. M. Órfão, M.F.R. Pereira Adsorption of anionic and cationic dyes on activated carbons with different surface chemistries, *Water Res.*, 38 (2004) 2043–2052.
- [24] S. Zavareh, A. Avanes, Effective and selective removal of aromatic amines from water by Cu²⁺-treated chitosan/alumina nanocomposite, *Adsorpt. Sci. Technol.*, 35 (2017) 218–240.
- [25] Q. Liu, L. Zhang, P. Hu, R. Huang, Removal of aniline from aqueous solutions by activated carbon coated by chitosan, *J. Water Reuse Desal.*, 5 (2015) 610–618.